Integrative and Comparative Biology, volume 50, number 6, pp. 950–966
doi:10.1093/icb/icq021

SYMPOSIUM

Photophysiology in Two Major Southern Ocean Phytoplankton Taxa: Photosynthesis and Growth of *Phaeocystis antarctica* and *Fragilariopsis cylindrus* under Different Irradiance Levels

Kevin R. Arrigo,[1,*] Matthew M. Mills,* Lindsey R. Kropuenske,* Gert L. van Dijken,* Anne-Carlijn Alderkamp* and Dale H. Robinson[†]

*Department of Environmental Earth System Science, 473 Via Ortega, Stanford University, Stanford, California 94305, USA; [†]Romberg Tiburon Center for Environment Studies, 3152 Paradise Drive, Tiburon, California 94920, USA

From the symposium "Advances in Antarctic Marine Biology" presented at the annual meeting of the Society for Integrative and Comparative Biology, January 3–7, 2010, at Seattle, Washington

[1]E-mail: arrigo@stanford.edu

Synopsis The Ross Sea, Antarctica, supports two distinct populations of phytoplankton, one that grows well in sea ice and blooms in the shallow mixed layers of the Western marginal ice zone and the other that can be found in sea ice but thrives in the deeply mixed layers of the Ross Sea. Dominated by diatoms (e.g. *Fragilariopsis cylindrus*) and the prymnesiophyte *Phaeocystis antarctica*, respectively, the processes leading to the development of these different phytoplankton assemblages are not well known. The goal of this article was to gain a better understanding of the photophysiological characteristics that allow each taxon to dominate its specific habitat. Cultures of *F. cylindrus* and *P. antarctica* were each grown semi-continuously at four different constant irradiances (5, 25, 65, and 125 μmol quanta/m^2/s). *Fragilariopsis cylindrus* produced far less photosynthetic pigment per cell than did *P. antarctica* but much more photoprotective pigment. *Fragilariopsis cylindrus* also exhibited substantially lower rates of photosynthesis and growth but also was far less susceptible to photoinhibition of cell growth. Excess photosynthetic capacity, a measure of the ability of phytoplankton to exploit variable light environments, was significantly higher in both strains of *P. antarctica* than in *F. cylindrus*. The combination of these characteristics suggests that *F. cylindrus* has a competitive advantage under conditions where mixed layers are shallow and light levels are relatively constant and high. In contrast, *P. antarctica* should dominate waters where mixed layers are deep and light levels are variable. These results are consistent with distributions of phytoplankton in the Ross Sea and suggest that light is the primary factor determining composition of phytoplankton communities.

Introduction

The Ross Sea is one of the most productive regions of the Southern Ocean, accounting for 25–30% of annual Southern Ocean primary production (Moore and Abbott 2000, Arrigo et al. 1998a, Arrigo et al. 2008). Because this region is covered by sea ice for much of the year, the bulk of annual production is restricted to austral spring and to summer blooms of phytoplankton that develop at the marginal ice zone (MIZ) and within polynyas (open water surrounded by ice) along the Victoria Land Coast and north of the Ross Ice Shelf. These blooms follow a predictable spatial and temporal pattern over the season of growth. In general, a large phytoplankton bloom forms by mid-November north of the Ross Sea Ice Shelf in the central Ross Sea Polynya and begins to decline by late December (Arrigo and McClain 1994, Arrigo et al. 1998a, Arrigo and Van Dijken 2004). Measurements taken in the field during the peak of these blooms have recorded surface chlorophyll *a* (Chl *a*) concentrations exceeding 10 mg/m^3 and

Advanced Access publication April 25, 2010

total accumulations of biomass >500 mg Chl *a*/m^2 (Smith and Gordon 1997; Arrigo et al. 1998b, 2000). Later, additional blooms develop in the western Ross Sea within the MIZ and within polynyas along the Victoria Land Coast in Terra Nova Bay and McMurdo Sound; these peak in January and begin to decline in February. Despite their delayed development, phytoplankton are in abundance in these blooms and can be at levels as high as those in the Ross Sea polynya (Arrigo et al. 2000). The annual bloom dynamics in these different regions have been linked to variations in stratification and mixed layer depth (MLD) that are driven by atmospheric forcing, in particular, to the strength and frequency of katabatic winds (Bromwich et al. 1992; Arrigo et al. 1998c).

Observations in the field from the Ross Sea have revealed that these spatially and temporally distinct blooms are strikingly different in terms of their phytoplankton species composition and hydrographic regime. Blooms of the prymnesiophyte *Phaeocystis antarctica* Karsten generally dominate the central Ross Sea polynya where surface waters are weakly stratified and deeply (40–60 m) mixed (DiTullio and Smith 1996; Arrigo et al. 1999, 2000). This species is also found in sea ice, but usually in relatively low numbers and mostly in association with newly formed ice near the Ross Sea polynya (Arrigo et al. 2003). Conversely, diatoms dominate the sea-ice microbial community as well as waters of the MIZ and coastal polynyas where surface stratification is intense and MLDs are shallow (<20 m).

The specific conditions that determine the distinct species composition of phytoplankton blooms in the southwestern Ross Sea are not well understood. The high correlation reported between species distribution and MLD suggests that diatoms are better adapted than *P. antarctica* to the higher irradiance characteristics of a shallow MLD, whereas *P. antarctica* is better adapted to low light levels and may be inhibited at high irradiance (Arrigo et al. 2000). However, field evidence to support this contention is equivocal (Van Hilst and Smith 2002; Robinson et al. 2003). Alternative hypotheses include species-specific differences in requirements for micronutrients, differences in the composition of pre-bloom phytoplankton seed populations, and differential rates of grazing by zooplankton (Van Hilst and Smith 2002). In addition, Robinson et al. (2003) suggested that the degree of variability of the light fields produced in deeply (more variable) and shallowly mixed (less variable) water columns, rather than the average irradiance of each hydrographic regime, may favor one taxonomic group over the other.

The importance of understanding control of the species composition of phytoplankton in the Southern Ocean lies in the very different biogeochemical and ecological roles played by different phytoplankton taxa within Antarctic marine systems. For example, *P. antarctica* is an important component of the marine sulfur cycle (Liss et al. 1994; DiTullio and Smith 1995), producing dimethylsulfoniopropionate (DMSP) in quantities that, when converted to volatile dimethyl sulfide, may contribute a substantial flux of biogenic sulfur to the atmosphere (Rhodes et al. 2009). Other evidence suggests that diatoms, which are central to the global silica cycle, are much more heavily grazed upon than is *P. antarctica* (Caron et al. 2000; Goffart et al. 2000; Tagliabue and Arrigo 2003). Ross Sea waters, dominated by diatoms and by *P. antarctica*, also differ markedly with respect to the trends in carbon and macronutrient drawdown ratios (Arrigo et al. 1999, 2000, 2002; Sweeney et al. 2000), and evidence from the field suggests that blooms of *P. antarctica* may be rapidly exported to the deep ocean and to sediments in the Ross Sea (DiTullio et al. 2000).

In this article, we present the photosynthetic responses of two phytoplankton taxa acclimated to a range of constant (nondynamic) growth irradiances to determine the extent to which taxon-specific responses to light influence the distribution of phytoplankton species in the Ross Sea. For this study, we chose the Antarctic diatom *Fragilariopsis cylindrus* Grunow and two strains of the Antarctic haptophyte *P. antarctica*, all of which are dominant bloom-forming organisms in the Southern Ocean. A better understanding of the factors controlling the composition and distribution of phytoplankton communities will provide the necessary framework from which to interpret past changes in these communities and to predict how these communities may change in the future in response to environmental perturbations.

Methods

Cultures

Nonaxenic cultures of *F. cylindrus* (CCMP 1102), *P. antarctica* (CCMP 1374), and *P. antarctica* (CCMP 1871), all isolated from the Southern Ocean, were obtained from the Provasoli-Guillard National Center for Culture of Marine Phytoplankton. Microalgae were grown in semi-continuous batch culture under continuous light at 2°C in synthetic ocean water (SOW) (Morel et al. 1979) enriched with F/2 macronutrients,

micronutrients, and vitamins (Price et al. 1989). The F/2 recipe for the *F. cylindrus* cultures was modified by increasing the $Si(OH)_4$ molar concentration to equal that of NO_3. The cultures were grown at four different irradiances (E_{gr}) of 5, 25, 65, and 125 μmol quanta/m^2/s. Growth was routinely monitored using *in vivo* chlorophyll fluorescence in a Turner Designs fluorometer (model 10-AU). Periodically, samples were taken for cell enumeration and for measurements of macronutrient and Chl *a* concentrations to ensure that the cultures were growing exponentially under nutrient-replete conditions.

After a minimum of 10 generations of growth under nutrient-replete conditions, the cultures were sampled in mid-exponential phase for measurements of photosynthetic characteristics, variable fluorescence, particulate absorption, macronutrient concentrations (nitrate and phosphate), cell abundance, particulate organic carbon (POC), Chl *a* concentration, and pigment complement.

Photosynthesis–irradiance incubations

Photosynthetic characteristics were obtained from photosynthesis–irradiance (P–E) measurements using a modification of the ^{14}C bicarbonate technique of Lewis and Smith (1983) as modified by Robinson et al. (1995). P–E incubations were carried out at 2°C and at 20 irradiances ranging from 0 to 635 μmol quanta/m^2/s. The incubator was an aluminum block containing illumination chambers to hold the incubation vials and channels through which coolant was continuously circulated. Even illumination was provided to each incubation chamber via a fiber-optic cable connected to an illuminator (Lumenyte International Corporation, model DMX512) fitted with a 150 W tungsten-halogen lamp. Total photosynthetically available radiation (PAR, 400–700 nm) within each illumination chamber was measured using a Spherical Micro Quantum Sensor US-SQS (Heinz Walz, GmBH). Spectral irradiance, $E(\lambda)$, was measured from 300–800 nm using a spectroradiometer (Analytical Spectral Devices, FieldSpec).

For each P–E curve, a 50-ml sample of stock culture was placed in a prechilled, 200-ml plastic beaker and spiked with 0.925 MBq $H^{14}CO_3$ to obtain a final activity of 0.019 MBq/ml. Total dissolved inorganic carbon concentration in each culture was 1.98 mmol/l. After thorough, but gentle, mixing, the spiked sample was distributed in 2-ml aliquots to 23 prechilled 20-ml plastic (polyethylene terephthalate) scintillation vials. Twenty of these vials were placed in individually illuminated chambers within the incubator and the incubation was initiated by turning on the light source. The contents of the three remaining vials (time-zero samples) were acidified with 100 μl of 6N HCl to drive off inorganic carbon and determine the background particulate radioactivity levels. To determine total radioactivity in the spiked sample, three 100-μl aliquots of spiked sample were added to scintillation vials containing 0.5 ml filtered seawater, 5 ml of scintillation fluid (EcoLume), and 100 μl of ethylamine and then assayed for radioactivity by liquid-scintillation counting (Perkin Elmer WinSpectral 1414). Incubations were terminated after 1 h by turning off the light source and adding 100 μl of 6N HCl to each vial. All acidified samples were gently shaken for a minimum of 12 h to drive off radioactive inorganic carbon and then neutralized with 100 μl of 6N NaOH and mixed with 10 μl of scintillation fluid. Radioactivity was determined by liquid-scintillation counting.

The P–E parameters were derived from a fit of P–E data to the equation of Platt et al. (1980)

$$P^* = P^*_s(1 - e^{-\alpha^* E/P^*_s})e^{-\beta^* E/P^*_s} - P^*_0 \qquad (1)$$

where P^* is the photosynthetic rate at irradiance E, P^*_s is the light-saturated photosynthetic rate in the absence of photoinhibition, α^* is the initial slope of the P–E curve, β^* is a measure of photoinhibition, and P^*_0 is the CO_2 uptake or release at $E = 0$ μmol quanta/m^2/s. The superscript * indicates that the term is normalized to Chl *a*. For POC-normalized parameters, the superscript * is replaced by *C*.

P^*_m, the maximum realized photosynthetic rate (photosynthetic capacity), was calculated as

$$P^*_m = P^*_s\left(\frac{\alpha^*}{\alpha^* + \beta^*}\right)\left(\frac{\beta^*}{\alpha^* + \beta^*}\right)^{\beta^*/\alpha^*}. \qquad (2)$$

The photoacclimation parameter E_k, is calculated as P^*_m/α^*.

Finally, excess photosynthetic capacity (EPC, Kana and Glibert 1987) was calculated as P^C_m/P^C_{Eg}, where P^C_{Eg} is the C-normalized productivity at the mean irradiance of the light treatment.

Particulate absorption

Specific absorption coefficients

Microalgae were filtered under low-vacuum pressure onto glass-fiber filters (Whatman GF/F) and particulate absorption spectra ($a_p(\lambda)$/m) were measured between wavelengths of 300 and 800 nm using a Perkin-Elmer Lambda 35 spectrophotometer following the method of Mitchell and Kiefer (1988). Detrital absorption spectra ($a_d(\lambda)$/m) were

determined for each $a_p(\lambda)$ spectra using the methanol extraction technique of Kishino et al. (1985). All $a_p(\lambda)$ and $a_d(\lambda)$ spectra were corrected for optical path amplification using the procedure of Mitchell and Kiefer (1988) and the coefficients of Bricaud and Stramski (1995). Chl *a*-specific phytoplankton absorption spectra ($a^*_{ph}(\lambda)$, m^2/mg Chl *a*) were calculated by subtraction of $a_d(\lambda)$ from $a_p(\lambda)$ (Roesler et al. 1989) and normalized to fluorometrically determined Chl *a* concentrations.

The spectrally weighted mean Chl *a*-specific absorption coefficient for phytoplankton ($\bar{a}^*$, m^2/mg Chl *a*) was calculated using the equation

$$\bar{a}^* = \frac{\sum_{400}^{700} a^*_{ph}(\lambda)E(\lambda)}{\sum_{400}^{700} E(\lambda)} \quad (3)$$

where $E(\lambda)$ (μmol quanta/m^2/s) is the spectral irradiance of the P–E incubator.

Determination of the maximum quantum yield of photosynthesis (Φ_m) depended upon the light level at which the maximum Φ_m was measured. Most models assume that Φ_m is achieved at the lowest irradiances, although this assumption does not always hold (Johnson and Barber 2003). Therefore, we first determined Φ at each photosynthetron light level (Φ_E) from $\bar{a}^*$ and the Chl *a*-normalized CO_2 uptake (P^*) using the equation presented by Johnson and Barber (2003)

$$\Phi_E = \frac{P^*_E}{43.2\bar{a}^* E} \quad (4)$$

where Φ_E is the calculated quantum yield of photosynthesis at each of the 20 irradiance levels (E) produced in the photosynthetron, P^*_E is the photosynthetic rate at irradiance E, and 43.2 is a unit conversion factor. When the assumption that Φ_m was maximal at the lowest light level was not met, Φ_m was chosen as the maximum value for Φ_E attained within the range of values of E used in the photosynthetron. When Φ_E was inversely related to irradiance, we calculated Φ_m using the equation

$$\Phi_m = \frac{\alpha^*}{43.2\bar{a}^*}. \quad (5)$$

Analysis of pigment

Duplicate samples for quantifying microalgal pigment composition were collected on glass fiber filters (Schleicher and Schuell GF/6) under low-vacuum pressure, placed in cryovials, and immediately flash-frozen in liquid nitrogen. Filters were then stored in a freezer at −80°C. Microalgal pigments were separated and quantified using high performance liquid chromatography (HPLC) using the method of Zapata et al. (2000).

Minor amounts of Chl *a* allomers, Chl *a*′, and chlorophyllides and phaeophytins of Chl *a*, were identified in most cultures. These Chl *a* derivatives were pooled with the measured Chl *a* and reported as total Chl *a*. The pigments of the xanthophyll cycle in *F. cylindrus* and *P. antarctica* consist of diadinoxanthin (DD) and diatoxanthin (DT). Interconversion between these two pigments within a cell involves an epoxidation or de-epoxidation step, with DT being the de-epoxidated form. The de-epoxidation state of the xanthophyll cycle was expressed as the amount of DT in a sample divided by the sum of DD and DT [i.e. DT/(DD + DT)].

Cell counts and growth rates

Aliquots (5 ml) of culture for each experiment were preserved in 2% gluteraldehyde and stored in the dark at 4°C. The samples were prepared by filtering 1–5 ml of preserved sample (volume depends on Chl *a* concentration at the time of collection) over polycarbonate filters (0.8 μm pore size) under mild vacuum pressure (<150 mm Hg). The 25-mm filter was then mounted on a glass slide using type FF immersion oil. At least 400 cells or 20 fields of view were counted under 100× magnification on a Leitz Laborlux 11 epifluorescence microscope. Growth rate (μ_{cell}) was determined from the slope of the best-fit of the natural logarithm of cell concentration over time, with R^2 always >0.94.

Growth versus irradiance curves, which are analogous to photosynthesis versus irradiance curves, were determined by plotting the cell-specific growth rate, μ_{cell}, against E_{gr} and fitting the relationship to the equation of MacIntyre et al. (2002) modified to include a parameter for photoinhibition of growth

$$\mu_{cell} = \mu^s_{cell}\left(1 - e^{-A_{gr}E_{gr}/\mu^s_{cell}}\right)e^{-B_{gr}E_{gr}/\mu^s_{cell}} \quad (6)$$

where μ^s_{cell} is the light-saturated growth rate in the absence of photoinhibition, A_{gr} is the initial slope of the growth-irradiance curve, and B_{gr} is the growth photoinhibition term. The maximum realized growth rate (μ^m_{cell}) is derived from

$$\mu^m_{cell} = \mu^s_{cell}\left(\frac{A_{gr}}{A_{gr}+B_{gr}}\right)\left(\frac{B_{gr}}{A_{gr}+B_{gr}}\right)^{B_{gr}/A_{gr}}. \quad (7)$$

The growth saturation parameter, K_E, is calculated as

$$K_E = \mu^m_{cell}/A_{gr}. \quad (8)$$

Variable fluorescence

Samples from microalgal cultures were placed in the dark at 2°C for at least 20 min prior to analysis of fluorescence. Preliminary tests showed no difference in results for dark adaptation times ranging from 20 min to 1 h. Four ml aliquots of the dark-adapted sample were added to a quartz glass cuvette and placed in the illumination chamber of a pulse amplitude modulated (PAM) fluorometer (Water PAM, Walz). Triplicate measurements of minimum (F_o) and maximum fluorescence (F_m) were taken and maximum potential photochemical efficiency of photosystem II (PSII) was calculated as F_v:F_m, where $F_v = F_m - F_o$.

POC

Duplicate samples for POC analysis were collected by filtering 10–25 ml of culture onto precombusted (450°C for 4 h) 2.5-cm glass-fiber filters (Whatman GF/F) under low pressure (<150 mm Hg). The vacuum was then released and 5 ml of 0.1N HCl was pipetted onto the filters and allowed to sit briefly to remove any inorganic C. The vacuum was then reapplied and the samples were rinsed with ~10 ml SOW. The samples were dried at 60°C and stored dry until analysis on a Carlo-Erba NA-1500 elemental analyzer.

Results

Pigments and the absorption of light

Photosynthetic pigments

The cellular content of virtually all photosynthetic pigments (chlorophylls and accessory pigments) in *F. cylindrus* and *P. antarctica* decreased as growth irradiance (E_{gr}) increased (Table 1). Cellular Chl *a* (pg/cell) decreased by ~4-fold, 2.5-fold, and 10-fold for *F. cylindrus*, *P. antarctica*-1871, and *P. antarctica*-1374, respectively, between the lowest (5 μmol quanta/m^2/s) and highest (125 μmol quanta/m^2/s) E_{gr} used in this study (Table 1). For *F. cylindrus*, the amount of primary accessory pigments (Chl *c* and fucoxanthin) were reduced to an even greater extent than was Chl *a* in response to higher E_{gr}, with the Chl *a*-normalized values (denoted by *) for Chl *c* (Chl *c**) and fucoxanthin (Fuco*) decreasing by 35 and 43%, respectively, between the lowest and highest E_{gr}. A similarly dramatic decrease in Chl *c**, Fuco*, and 4-keto-19'-hexanoyloxyfucoxanthin* (Keto*) was observed with increasing growth irradiance in *P. antarctica*-1871. In contrast, changes in the most abundant photosynthetic xanthophyll pigment in this species, 19' hexanoyloxyfucoxanthin (19-Hex), roughly paralleled that of Chl *a*, resulting in Chl *a*-normalized values that exhibited little, or no, relationship with growth irradiance. The accessory pigments of *P. antarctica*-1374 also exhibited decreasing trends with increasing E_{gr} that approximately paralleled the trend in Chl *a*, with the exception of Fuco* and Keto*, which were significantly enhanced in cultures grown at 5 μmol quanta/m^2/s, compared to those grown at higher irradiance. Nevertheless, the content of Chl *a*-normalized accessory pigment for this strain was not significantly correlated with E_{gr}.

Absorption

The increased pigment content per cell that accompanies acclimation to low irradiance leads to an overall increase in the cellular absorption cross-section, thereby increasing the probability of photon absorption by the cell. However, this increased aggregation of pigments within cells is often observed as a decrease in a^*_{ph}, due to less

Table 1 Cellular Chl *a* (pg/cell) and accessory-pigment composition presented as Chl *a*-normalized values (denoted with asterisks) of *F. cylindrus* and *P. antarctica* at four growth irradiances (E_{gr}, μmol quanta/m^2/s)

	E_{gr}	Chl *a*	Chl *c**	But*	Fuco*	Keto*	Hex*	DD+DT*	DT/(DD+DT)
Fragilariopsis cylindrus-1102	5, $n=3$	0.19 (0.11)	0.202 (0.011)	ND	0.389 (0.053)	ND	ND	0.034 (0.009)	0.296 (0.101)
	25, $n=2$	0.18 (0.13)	0.149 (0.023)	ND	0.322 (0.001)	ND	ND	0.098 (0.038)	0.448 (0.136)
	65, $n=9$	0.05 (0.01)	0.149 (0.025)	ND	0.274 (0.098)	ND	ND	0.166 (0.058)	0.588 (0.124)
	125, $n=9$	0.05 (0.01)	0.132 (0.031)	ND	0.222 (0.128)	ND	ND	0.179 (0.055)	0.711 (0.067)
Phaeocystis antarctica-1871	5, $n=11$	0.25 (0.05)	0.267 (0.051)	0.007 (0.006)	0.081 (0.035)	0.035 (0.10)	0.117 (0.22)	0.023 (0.007)	0.226 (0.098)
	25, $n=5$	0.17 (0.04)	0.244 (0.078)	0.009 (0.010)	0.042 (0.046)	0.031 (0.025)	0.176 (0.109)	0.031 (0.025)	0.209 (0.132)
	65, $n=12$	0.16 (0.03)	0.189 (0.065)	0.011 (0.006)	0.034 (0.024)	0.013 (0.006)	0.122 (0.041)	0.038 (0.033)	0.395 (0.154)
	125, $n=12$	0.10 (0.02)	0.153 (0.045)	0.008 (0.004)	0.022 (0.014)	0.010 (0.004)	0.101 (0.030)	0.032 (0.010)	0.520 (0.110)
Phaeocystis antarctica-1374	5, $n=3$	1.55 (0.21)	0.218 (0.015)	0.000 (0.000)	0.079 (0.019)	0.028 (0.004)	0.074 (0.011)	0.015 (0.001)	0.071 (0.075)
	25, $n=3$	0.34 (0.02)	0.204 (0.033)	0.002 (0.000)	0.028 (0.005)	0.011 (0.004)	0.126 (0.027)	0.014 (0.003)	0.174 (0.163)
	65, $n=3$	0.17 (0.03)	0.195 (0.018)	0.002 (0.001)	0.016 (0.002)	0.010 (0.002)	0.115 (0.022)	0.012 (0.005)	0.189 (0.177)
	125, $n=5$	0.14 (0.01)	0.226 (0.058)	0.003 (0.004)	0.029 (0.056)	0.013 (0.017)	0.111 (0.028)	0.014 (0.008)	0.236 (0.042)

Shown are mean and (SD). Ratios <0.005 are reported as not detected (ND).

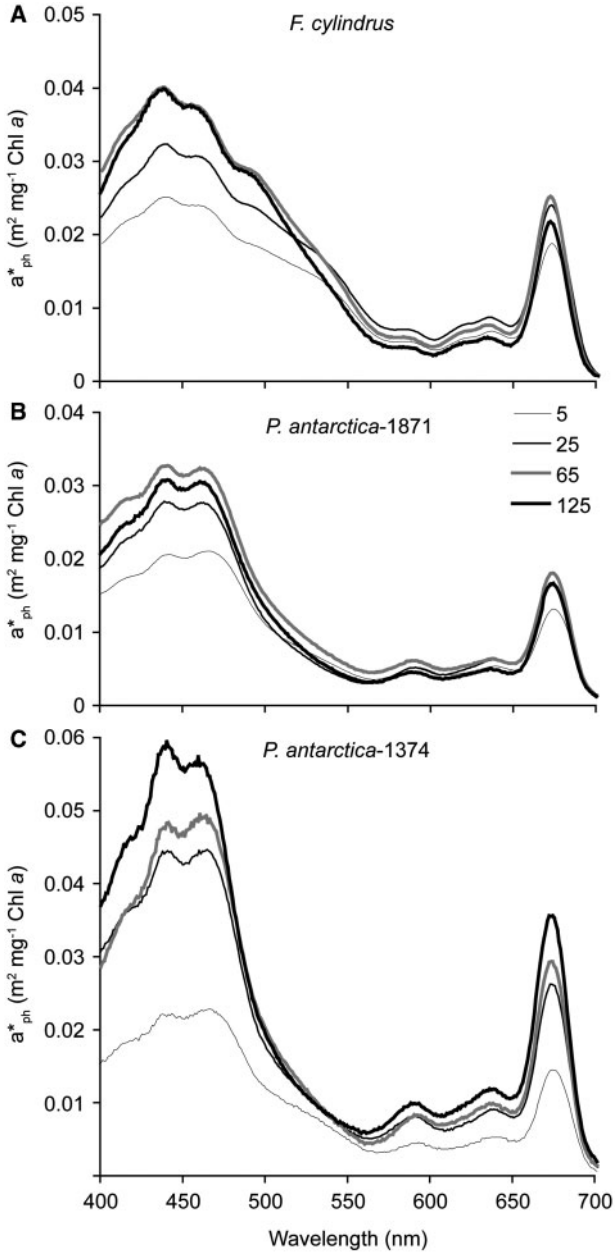

Fig. 1 Absorption spectra of phytoplankton, a^*_{ph}, for (**A**) *F. cylindrus*, (**B**) *P. antarctica*-1871, and (**C**) *P. antarctica*-1374, grown at 5, 25, 65, and 125 μmol quanta/m^2/s.

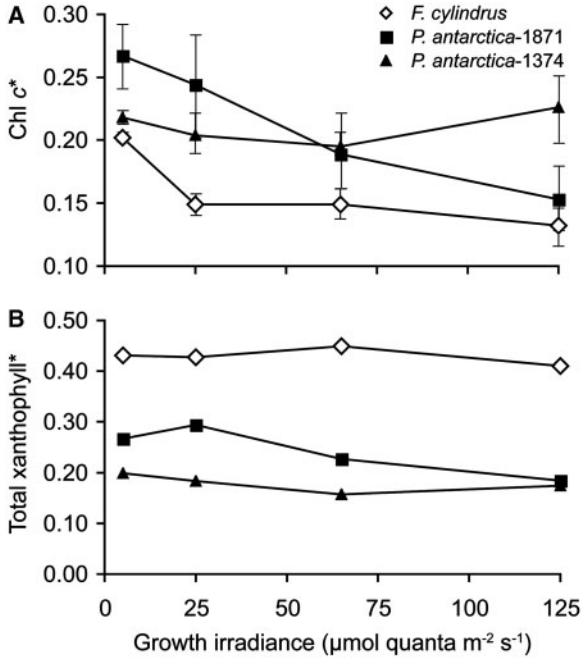

Fig. 2 E_{gr} versus (**A**) Chl *a*-normalized total Chl *c* (Chl c_1+Chl c_2+Chl c_3) and (**B**) Chl *a*-normalized total xanthophyll pigments (But+Fuco+Keto+Hex+DD+DT+β-Car). The asterisk denotes normalization by Chl *a*. Shown are mean ± SD; in some cases the SD is smaller than the size of the datum symbol.

efficient absorption per mass of pigment, a consequence of pigment packaging (Morel and Bricaud 1981). This phenomenon is stronger at wavelengths with higher absorption coefficients (400–500 nm), thereby resulting in a flattening of the absorption spectra as intracellular pigment concentrations and/or cell size increases. The a^*_{ph} spectra for *F. cylindrus* (Fig. 1A) and *P. antarctica*-1871 (Fig. 1B) exhibited a modest decrease with lower E_{gr} that is most obvious in the blue regions of the spectrum, characteristic of pigment packaging. Pigment packaging was even more pronounced in *P. antarctica*-1374 (Fig. 1C), where a^*_{ph} increased nearly 3-fold in the blue region of the spectrum between the E_{gr} of 5 and 125 μmol quanta/m^2/s.

Differences in the patterns of the a^*_{ph} spectra reflect differences in the concentration of pigment in the phytoplankton. Both strains of *P. antarctica* exhibited a strong secondary absorption peak in the blue region of the spectrum (450–470 nm) that was nearly equal to, or greater than, the blue (443 nm) Chl *a* absorption peak (Fig. 1B and C). Because Chl *c** was consistently higher for both strains of *P. antarctica* than for *F. cylindrus* at corresponding values for E_{gr} (Fig. 2A), the likely source of this enhanced blue absorption is the Chl *c* pigments, which absorb strongly at these wavelengths (Bidigare et al. 1986). In addition, *F. cylindrus* (Fig. 1A) exhibited greater absorption in the green region of the spectrum (500–575 nm) than did either strain of *P. antarctica*. This region of enhanced absorption corresponds to wavelengths at which Fuco and the photoprotective xanthophyll pigments contribute significantly to absorption in diatoms. At the E_{gr} levels used in this study, total xanthophyll pigment relative to Chl *a* was 45–186% greater in *F. cylindrus* than in *P. antarctica* (Fig. 2B) and is the likely source of enhanced absorption in the green region of the a^*_{ph} spectra of *F. cylindrus*.

Surprisingly, the mean Chl *a*-specific absorption coefficient ($\bar{a}^*$) exhibited no significant trend with E_{gr} for either *F. cylindrus* or *P. antarctica*-1871 (Table 2). This somewhat nonintuitive observation is likely a consequence of the spectral characteristics of the P–E incubator's light source and differences in accessory pigments between the three algal cultures. The spectral output of the light source was greatest at 500–600 nm, the region of the a^*_{ph} spectrum where phytoplankton absorption is relatively low and hence any changes due to pigment packaging will be small. Because this incubator light spectrum is used to weight the calculation of $\bar{a}^*$ (Equation 3), the sensitivity of the parameter $\bar{a}^*$ to pigment packaging will be reduced. More importantly, as noted above, the cellular concentration of photosynthetic accessory pigments in both *F. cylindrus* and *P. antarctica*-1871 increased even more dramatically than did Chl *a* in response to decreasing E_{gr}. Consequently, the decrease in light absorption per unit Chl *a* that usually accompanies an increase in Chl *a* per cell (i.e. pigment packaging) at lower irradiances was compensated by increased light absorption by accessory pigments. As a result, $\bar{a}^*$ was not diminished at the lower treatments with E_{gr}. In contrast, intracellular concentrations of accessory pigments in *P. antarctica*-1374 also increased with decreasing E_{gr}, but were approximately proportional to changes in Chl *a* concentration. Therefore, light absorption per unit Chl *a* dropped markedly with decreases in E_{gr} for *P. antarctica*-1374, resulting in the observed reduction in $\bar{a}^*$.

Pigments of the xanthophyll cycle

Nonphotochemical quenching (NPQ), or thermal dissipation of excitation energy via pigments of the xanthophyll cycle is a rapid photoprotective response (Olaizola and Yamamoto 1994; Olaizola et al. 1994). In both diatoms and *Phaeocystis*, the xanthophyll cycle is represented by the reversible light-driven conversion of the epoxide pigment, DD, into the epoxide-free (de-epoxidated) form, DT. In *F. cylindrus*, total DD+DT normalized to Chl *a* (DD+DT*) increased markedly in response to higher E_{gr}, with values >5-fold greater at the highest E_{gr} than at the lowest (Table 1 and Fig. 3A). DD+DT* represented a major component by weight of the pigments of *F. cylindrus* at the highest E_{gr}, exceeding the contribution of total Chl *c** and nearly matching the contribution of Fuco* (Table 1). Conversely, DD+DT* exhibited no change with E_{gr} in either strain of *P. antarctica* and was consistently lower than corresponding values for *F. cylindrus*.

The fraction of total pigment of the xanthophyll cycle present in the photoprotective, de-epoxidated form also increased in *F. cylindrus* at higher E_{gr}, with DT increasing from 30% of total xanthophyll-cycle pigments [DT/(DD+DT)] at 5 μmol quanta/m^2/s to 71% at 125 μmol quanta/m^2/s (Table 1 and Fig. 3B). However, DT/(DD+DT) also increased with E_{gr} in both strains of *P. antarctica*, although not to the same degree as *F. cylindrus* (Fig. 3B), indicating that although the content of xanthophyll-cycle pigments was relatively low, the xanthophyll cycle was being used by *P. antarctica* as a photoprotective mechanism in high light.

Photosynthetic parameters

F_v:F_m

In all three phytoplankton cultures, F_v:F_m dropped slightly with increasing irradiance (Table 2), with the largest drop being exhibited by *F. cylindrus* (25% between 5 and 125 μmol quanta/m^2/s) and the smallest by *P. antarctica*-1871 (12%). In addition, F_v:F_m was ~20–35% higher at each E_{gr} in both strains of *P. antarctica* than in *F. cylindrus*.

C:Chl *a*

The C:Chl *a* (g:g) ratio rose significantly with increasing E_{gr} in all three phytoplankton taxa, with those cultures growing at 125 μmol quanta/m^2/s exhibiting values ~4-fold higher than those at 5 μmol quanta/m^2/s (Table 2). This increase in C:Chl *a* with E_{gr} was attributable primarily to corresponding decreases in Chl *a*/cell observed in all culture isolates, since C/cell was much less variable with light (Table 2). The C:Chl *a* ratios for both *P. antarctica*-1871 and *P. antarctica*-1374 were 2- and 3-fold greater, respectively, than those of *F. cylindrus* at all levels of E_{gr}. This is explained by much higher C/cell in *P. antarctica* cultures compared with *F. cylindrus*, although C/cell in *P. antarctica*-1374 significantly exceeded that of *P. antarctica*-1841.

Photosynthetic capacity

Despite similar values for F_v:F_m, *F. cylindrus* and *P. antarctica* differed markedly in their ability to adjust their photosynthetic capacity in response to changes in E_{gr} (Table 2). For *F. cylindrus*, Chl *a*-normalized photosynthetic capacity (P^*_m) was relatively low compared to *P. antarctica* and invariant over the wide range of E_{gr} used in this study (5–125 μmol quanta/m^2/s), ranging only from 0.44 to 0.54 mg C/mg Chl *a*/h. In contrast, P^*_m in both strains of *P. antarctica* was much greater and exhibited a significant positive trend with E_{gr}, increasing

Table 2 Photosynthetic characteristics of *F. cylindrus* and *P. antarctica* acclimated to four different growth irradiances (E_{gr}), including Chl *a*-normalized and C-normalized P–E parameters.

E_{gr}	F_v:F_m	C:Chl *a*	C/cell	P_m^*	α^*	β^*	E_k	Φ_m	$\bar{a}^*$	P_m^C	α^C	β^C	μ_{cell}
Fragilariopsis cylindrus-1102													
5, $n=11$	0.59 (0.04)	25 (10)	4.75	0.46 (0.36)	0.042 (0.029)	6.3e-4 (6.6e-4)	12 (3)	0.057 (0.028)	0.012 (0.002)	0.41 (0.37)	0.037 (0.031)	6.1e-4 (6.9e-4)	0.06 (0.01)
25, $n=5$	0.54 (0.04)	44 (13)	7.92	0.44 (0.02)	0.043 (0.015)	4.8e-4 (2.1e-4)	11 (4)	0.042 (0.006)	0.014 (0.002)	0.26 (0.09)	0.040 (0.021)	3.3e-4 (2.3e-4)	0.10 (0.01)
65, $n=12$	0.45 (0.04)	89 (51)	4.45	0.54 (0.50)	0.031 (0.029)	5.4e-4 (6.4e-4)	19 (7)	0.032 (0.013)	0.013 (0.002)	0.17 (0.11)	0.011 (0.009)	1.8e-4 (1.2e-4)	0.11 (0.06)
125, $n=12$	0.44 (0.03)	96 (37)	4.80	0.54 (0.16)	0.014 (0.005)	4.5e-4 (3.9e-4)	42 (14)	0.016 (0.006)	0.014 (0.002)	0.15 (0.06)	0.004 (0.002)	1.3e-4 (1.2e-4)	0.09 (0.02)
Phaeocystis antarctica-1871													
5, $n=3$	0.70 (0.01)	41 (14)	10.3	1.4 (0.3)	0.038 (0.008)	7.6e-4 (4.5e-4)	37 (8)	0.100 (0.022)	0.0088 (0.002)	0.85 (0.23)	0.023 (0.008)	5.9e-4 (5.1e-4)	0.07 (0.01)
25, $n=3$	0.67 (0.03)	103 (30)	17.5	2.7 (0.4)	0.060 (0.011)	3.0e-4 (1.4e-4)	45 (3)	0.101 (0.015)	0.0094 (0.001)	0.66 (0.34)	0.015 (0.009)	6.0e-5 (4.0e-5)	0.12 (0.02)
65, $n=9$	0.61 (0.04)	121 (42)	19.4	3.5 (0.8)	0.074 (0.013)	-1.7e-5 (5.1e-4)	48 (10)	0.086 (0.020)	0.011 (0.005)	0.76 (0.17)	0.017 (0.007)	1.0e-5 (1.2e-4)	0.25 (0.01)
125, $n=9$	0.61 (0.03)	190 (96)	19.0	5.0 (2.2)	0.061 (0.014)	7.4e-4 (7.4e-4)	78 (19)	0.083 (0.011)	0.010 (0.003)	0.57 (0.08)	0.008 (0.002)	7.0e-5 (1.0e-4)	0.22 (0.05)
Phaeocystis antarctica-1374													
5, $n=3$	0.68 (0.01)	66 (10)	75.9	1.7 (0.3)	0.064 (0.010)	6.4e-4 (3.0e-4)	26 (1)	0.115 (0.006)	0.0085 (0.002)	0.62 (0.17)	0.023 (0.006)	2.4e-4 (1.4e-4)	0.09 (0.02)
25, $n=3$	0.64 (0.01)	130 (20)	44.2	3.4 (0.4)	0.090 (0.006)	1.2e-3 (3.0e-4)	37 (3)	0.089 (0.014)	0.0146 (0.002)	0.63 (0.16)	0.017 (0.034)	2.2e-4 (2.0e-5)	0.30 (0.03)
65, $n=3$	0.55 (0.02)	171 (54)	29.1	4.1 (1.0)	0.099 (0.022)	1.8e-3 (1.1e-3)	43 (1)	0.080 (0.003)	0.0157 (0.005)	0.78 (0.28)	0.019 (0.006)	3.3e-4 (2.2e-4)	0.35 (0.13)
125, $n=3$	0.54 (0.01)	284 (23)	39.8	6.4 (0.3)	0.11 (0.019)	1.6e-3 (7.7e-4)	60 (7)	0.089 (0.033)	0.0181 (0.005)	0.66 (0.17)	0.011 (0.003)	1.7e-4 (1.2e-4)	0.22 (0.04)

Shown are means and (SD). Units: P_m^* = mg C/mg Chl *a*/h; α^* and β^* = mg C/mg Chl *a*/h (μmol quanta/m^2/s]$^{-1}$; E_{gr} and E_k = μmol quanta/m^2/s; Φ_C = mol C/mol quanta; F_v:F_m is dimensionless; $\bar{a}^*$ = m^2/mg Chl *a*; $P_m^C = d^{-1}$; α^C and $\beta^C = d^{-1}$ (μmol quanta/m^2/s)$^{-1}$; μ_{cell} = d^{-1}; C/cell = pg/cell.

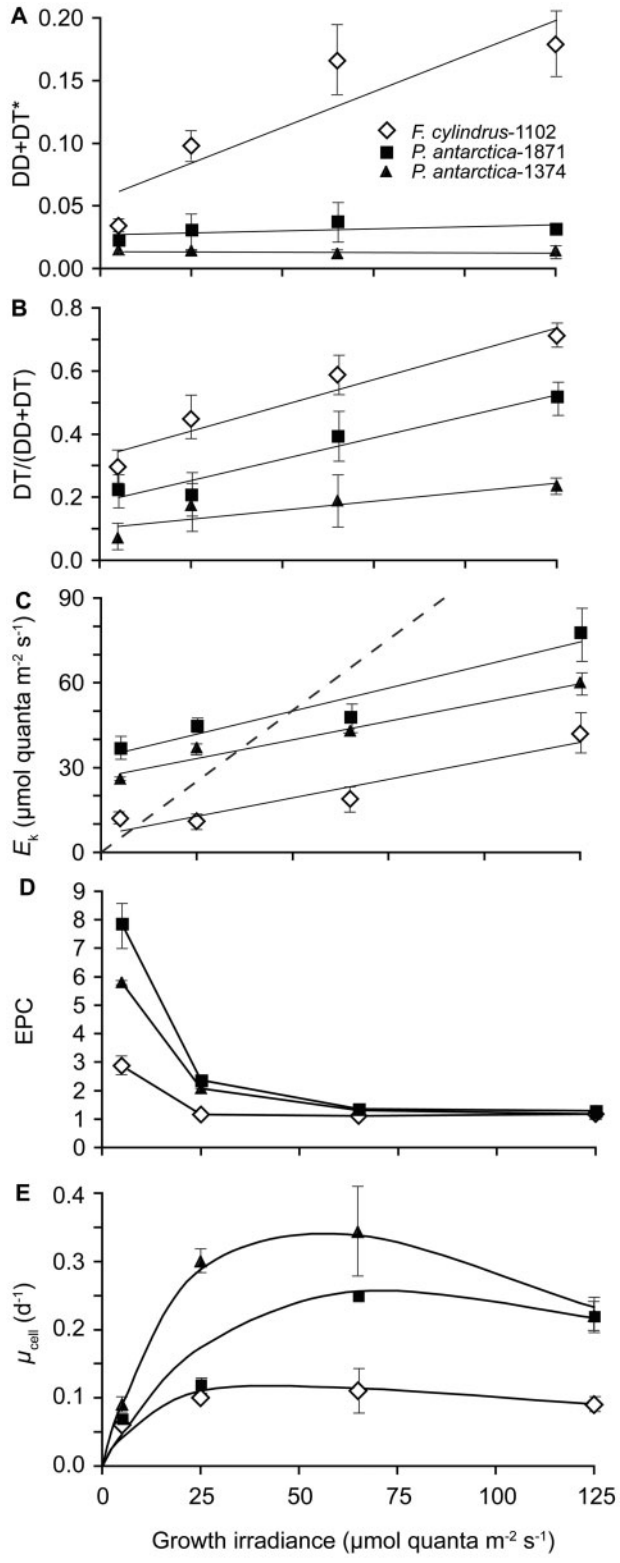

Fig. 3 Growth irradiance (E_{gr}) versus: (**A**) Xanthophyll cycle pigment content normalized to Chl *a* (DD+DT*). (**B**) The fraction of total xanthophyll cycle pigment that is in the de-epoxidated form [DT/(DD+DT)]; lines represent linear regression to the data. (**C**) The photoacclimation index (E_k); the dashed line denotes a one-to-one relationship. (**D**) EPC. Shown are mean ± SD; in some cases the SD is smaller than the size of the datum symbol. (**E**) Cell-specific growth rate (μ_{cell}); the lines represent the best fit to Equation 6 and are significant at the 95% confidence level.

from 1.4 to 1.7 mg C/mg Chl *a*/h at 5 μmol quanta/m^2/s to 5.0–6.4 mg C/mg Chl *a*/h at the highest growth irradiance of 125 μmol quanta/m^2/s.

Interestingly, these taxon-specific trends with E_{gr} changed when photosynthetic capacity was normalized by cellular C (P^*_m) rather than by Chl *a*. Normalization of P_m by C provides an estimate of the C-specific growth rate (i.e. g C/g C/h, or more simply per hour). In this case, P^*_m in *F. cylindrus* decreased with increasing E_{gr}, dropping from 0.41/d at 5 μmol quanta/m^2/s to 0.15/d at 125 μmol quanta/m^2/s, while *P. antarctica* exhibited no significant change in P^C_m with E_{gr} (Table 2). Both strains of *P. antarctica* exhibited higher values of P^C_m (0.57–0.85/d) than *F. cylindrus*, but the differences between taxa (2- to 5-fold) were not nearly as large as they were for P^*_m (3- to 11-fold) due to the larger C:Chl *a* of both *P. antarctica* strains.

Photosynthetic efficiency

Changes in the Chl *a*-normalized photosynthetic efficiency (α^*) with E_{gr} also differed substantially between taxa (Table 2). Generally, α^* is inversely related to irradiance, since it is beneficial for algae growing at low light to maximize their photosynthetic efficiency. This inverse relationship between α^* and light stems from the fact that, although α^* is proportional to both the quantum yield of photosynthesis (Φ_m, which is negatively correlated with light) and $\bar{a}^*$ (which is positively correlated with light), changes in Φ_m are usually larger than changes in $\bar{a}^*$ for a corresponding change in light. Hence, α^* usually increases as light diminishes (see Equation 5 for the relationship between α^*, $\bar{a}^*$, and Φ_m).

Fragilariopsis cylindrus exhibited the expected decreasing trend in α^* at progressively higher E_{gr} (Table 2), falling from 0.042 mg C/mg Chl *a*/h (μmol quanta/m^2/s)$^{-1}$ at 5 μmol quanta/m^2/s to 0.014 mg C/mg Chl *a*/h (μmol quanta/m^2/s)$^{-1}$ at 125 μmol quanta/m^2/s. This decrease was not the result of reduced harvesting of light at higher growth irradiance, since $\bar{a}^*$ showed virtually no variation in response to E_{gr} (Table 2). Instead, nearly all of the variability in α^* was attributable to decreases in Φ_m, which fell from 0.057 at the lowest E_{gr} to 0.016 at the highest (Table 2). This pattern of α^* with E_{gr} contrasts markedly with that of *P. antarctica*, which exhibited either no significant trend (strain 1871) or a slight increase in α^* with E_{gr} (strain 1374). In both *P. antarctica* strains, Φ_m decreased at higher values of E_{gr}, although the changes were quite small (23%) compared to those exhibited by *F. cylindrus* (72%). Furthermore, values for Φ_m exhibited by both strains of *P. antarctica* were

surprisingly high at all levels of E_{gr}, in many cases approaching the theoretical maximum value of 0.125 (Table 2). These high quantum yields are typical for Ross Sea phytoplankton communities in summer (Vaillancourt et al. 2003). The lack of a trend in α^* with E_{gr} in *P. antarctica*-1871 can be attributed to the fact that neither $\bar{a}^*$ nor Φ_m exhibited a strong pattern with E_{gr} (α^* is proportional to both Φ_m and a^*_{ph}). The more unusual increase in α^* with increasing E_{gr} in *P. antarctica*-1374 was due to the large increase in $\bar{a}^*$, which swamped the relatively small corresponding decrease in Φ_m.

When normalized by C, the photosynthetic efficiency (α^C) exhibited the expected decrease with increasing E_{gr} in all three taxa of phytoplankton (Table 2). The two strains of *P. antarctica* exhibited similar values of α^C, decreasing from 0.023/d (μmol quanta/m^2/s) $^{-1}$ at 5 mol quanta/m^2/s to 0.008–0.011/d (μmol quanta/m^2/s)$^{-1}$ at 125 μmol quanta/m^2/s. Values of α^C were much more variable as a function of E_{gr} in *F. cylindrus*, decreasing ~10-fold from a relatively high value of 0.037/d (μmol quanta/m^2/s)$^{-1}$ at 5 μmol quanta/m^2/s to 0.004/d (μmol quanta/m^2/s)$^{-1}$ at 125 μmol quanta/m^2/s.

Photoacclimation parameter

The photoacclimation parameter, E_k (μmol quanta/m^2/s) represents the light level at which rates of light absorption are in approximate energetic balance with rates of CO_2 fixation. In general, well-acclimated phytoplankton will exhibit values for E_k that are consistent with the mean light field under which they were growing. Consistent with this pattern, E_k increased with E_{gr} for all three taxa (Table 2 and Fig. 3C). The E_k for *F. cylindrus* ranged from 12 to 42 μmol quanta/m^2/s, although E_k was of similar magnitude to E_{gr} only for $E_{gr} = 5$ μmol quanta/m^2/s. As a consequence of this limited response to E_{gr}, *F. cylindrus* was well acclimated to only the lowest E_{gr} used in this study. At higher E_{gr}, cultures of *F. cylindrus* were growing under conditions of illumination that were supersaturating for photosynthesis (i.e. $E_k < E_{gr}$).

Unlike *F. cylindrus*, both strains of *P. antarctica* exhibited variability in P^*_m and α^* that also resulted in an increase in E_k in response to higher E_{gr} (Table 2). However, E_k increased only 2-fold between treatments with light at 5 and 125 μmol quanta/m^2/s, despite a 25-fold increase in E_{gr}. At the lower values for E_{gr} (5–25 μmol quanta/m^2/s), E_k exceeded E_{gr}, indicating that photosynthetic rates saturated at irradiance levels greatly in excess of E_{gr}. However, under higher E_{gr} conditions (65–125 μmol quanta/m^2/s), irradiance was super-saturating for photosynthesis for both strains of *P. antarctica* ($E_k < E_{gr}$, Fig. 3C).

EPC

EPC (Fig. 3D) characterizes the capacity for phytoplankton to increase fixation of CO_2 when exposed to high irradiance (Kana and Glibert 1987). High values are indicative of an ability to exploit variable light regimes such that when irradiance is high (i.e. when phytoplankton are mixed to the surface), phytoplankton can increase their photosynthetic rates and take advantage of the additional light energy. EPC declined with E_{gr} in all three taxa, reaching a minimum at 65 μmol quanta/m^2/s (Fig. 3D). However, *F. cylindrus* exhibited the lowest EPC values, particularly at low E_{gr}, suggesting that this species is not well suited to variable light regimes.

Photoinhibition

The photoinhibition parameter, β^*, exhibited no obvious trend with E_{gr} for either *F. cylindrus* or *P. antarctica*-1871 (Table 2). For *P. antarctica*-1374, β^* expressed the unusual pattern of being lower at 5 and 25 μmol quanta/m^2/s than at 65 and 125 μmol quanta/m^2/s, although the differences were not significant. However, when β was normalized by C (β^C), the positive trend with E_{gr} disappeared for *P. antarctica*-1374 (no trend) while the β^C for both *F. cylindrus* and *P. antarctica*-1871 decreased with increasing E_{gr} (Table 2), although variability was high and the differences were not significant. This decrease in β^C at higher values for E_{gr} suggests that photodamage was reduced in cultures of phytoplankton photoacclimated to higher irradiance. This effect is not seen in β^* because the decrease in Chl *a*/cell at high E_{gr} was likely larger than the increase in photoinhibition, which resulted in β^* either not changing or increasing at high E_{gr}.

Growth rates

Cell-specific grow rates (μ_{cell}) ranged from 0.06–0.11/d, 0.07–0.25/d, and 0.09–0.35/d for *F. cylindrus*, *P. antarctica*-1871, and *P. antarctica*-1374, respectively, when cultures were grown at E_{gr} between 5–125 μmol quanta/m^2/s (Fig. 3E). These rates are lower than those reported for cultures of *F. cylindrus* and *P. antarctica* grown at 0°C (0.69/d and 0.71/d, respectively) by Sommer (1989) but within the range found for *F. cylindrus*-dominated (0.02–0.23/d) and *P. antarctica*-dominated (0.04–1.02/day) waters of the Ross Sea during the austral spring (Smith et al. 1999).

Fragilariopsis cylindrus and *P. antarctica* exhibited similar values for μ_{cell} at the lowest growth

Table 3 Growth rate parameters of *F. cylindrus*, *P. antarctica*-1871 and *P. antartica*-1374 derived as a function of E_{gr} using data shown in Fig. 3E

	K_E	μ^s_{cell}	A_{gr}	B_{gr}	μ^m_{cell}	E_b
Fragilariopsis cylindrus-1102	7.02	0.15	0.019	0.0006	0.13	250
Phaeocystis antarctica-1841	25.7	0.85	0.010	0.0074	0.26	113
Phaeocystis antarctica-1374	17.9	0.80	0.020	0.0076	0.36	107

irradiance ($E_{gr} = 5\,\mu$mol quanta/m^2/s). However, at $E_{gr} \geq 25\,\mu$mol quanta/m^2/s, the growth rate was ~2-fold higher for *P. antarctica*-1871 and 3-fold higher for *P. antarctica*-1374 (Fig. 3E). Furthermore, parameters derived from the growth–irradiance relationship (Equations 6–8) revealed three important results (Table 3). First, the maximum growth rate of *P. antarctica* in the absence of photoinhibition (μ^s_{cell}) was five to six times higher than in *F. cylindrus*. Even taking photoinhibition into account, the maximum growth rate (μ^m_{cell}) of *P. antarctica* exceeded that of *F. cylindrus* by 2- to 3-fold. Second, K_E (the light level where growth rate begins to flatten) in *F. cylindrus* was only 27% of that of *P. antarctica*-1871 and 40% of that of *P. antarctica*-1374, suggesting that growth of *F. cylindrus* saturates at a lower irradiance than that of *P. antarctica*. Finally, growth rates for both strains of *P. antarctica* were much more strongly inhibited at higher irradiance than those of *F. cylindrus*, exhibiting values for B_{gr} (parameter describing photoinhibition of cell growth) that were 12.5-fold greater than that observed for *F. cylindrus*. Calculated values for the photoinhibition index ($E_b = B_{gr}/\mu_{cell}$) for these three taxa indicate that both strains of *P. antarctica* are twice as prone to photoinhibition as *F. cylindrus* (Table 3).

Discussion

Photoacclimation in *F. cylindrus* and *P. antarctica*

Photoacclimation in phytoplankton consists of a suite of coordinated adjustments in photophysiology and chemical composition that balances the acquisition of light energy with the capacity to use that energy for CO_2-fixation and other metabolic processes. For phytoplankton exposed to low mean irradiance, the major challenge is to obtain enough energy for survival and growth from the limited light resource. Common photoacclimation responses for phytoplankton growing under low light include increasing the ability to harvest energy from the ambient light field and reducing energetic costs for cell maintenance and growth. At high mean irradiance, responding appropriately to excess light energy and its potentially damaging effects on PSII is of particular importance. Typically, acclimation involves reducing harvesting of light and up-regulating mechanisms that dissipate or divert excess energy.

In this study, all three types of phytoplankton cultures exhibited changes in light-harvesting potential when they were grown under a range of static irradiance regimes. We observed a progressive decrease in Chl *a* and most photosynthetic accessory pigments, normalized to both cell number and particulate C, as E_{gr} increased. In addition, it is likely that actual light-harvesting potential was reduced at higher E_{gr} due to high concentrations of photoprotective pigments, which compete with photosynthetic pigments for the absorption of available photons but do not transfer the absorbed energy to photosynthetic pathways. The changes in pigmentation exhibited by our phytoplankton cultures, which enhance acquisition of light energy at lower irradiance and reduce acquisition and the potential for photodamage at higher irradiance, are consistent with photoacclimation responses typically observed for phytoplankton.

All three phytoplankton strains were grown under conditions of illumination that were saturating to growth: *F. cylindrus* at $E_{gr} > 5\,\mu$mol quanta/m^2/s and both *P. antarctica* strains at $E_{gr} > 25\,\mu$mol quanta/m^2/s. The likely outcome of chronic exposure to saturating irradiance is for the phytoplankton initially to display symptoms of photoinhibition and, in response, to employ photoprotective mechanisms that reduce excitation pressure on PSII. Our study provides several indicators of photoinhibition and photoprotection, including β^*, DD+DT*, trends with E_{gr} in F_v:F_m (a measure of the maximum potential photochemical efficiency of PSII), and Φ_m (a measure of the number of moles of CO_2 reduced for each mole of quanta absorbed). F_v:F_m is measured after a period of dark acclimation during which NPQ of the chlorophyll fluorescence due to the xanthophyll cycle is presumed to relax completely. Any reduction in F_v:F_m from the highest values observed for unstressed phytoplankton has often been attributed to deactivation of reaction centers due to environmental stress such as limitation of growth by inadequate nutrient supply and photoinhibitory damage due to super-saturating irradiance. Φ_m is derived from measurements of light absorption and radiolabeled CO_2 fixation. Therefore, anything that diverts absorbed photon equivalents from the pathway to gross C reduction will reduce Φ_m, including NPQ due to the xanthophyll cycle and other photoprotective mechanisms that provide alternate electron sinks downstream of PSII. A significant decrease in F_v:F_m was observed for both strains

of *P. antarctica* (Table 2), with values at the highest E_{gr} being 13–20% lower than those at lowest E_{gr}, indicating that although exposure to supersaturating irradiance stressed the photosynthetic apparatus, most of the functionality of PSII (i.e. 80–87% of photochemical efficiency) was preserved. The corresponding decrease in Φ_m (values at the highest E_{gr} were lower by 17–23% compared to those at lowest E_{gr}) was of similar magnitude to that observed for F_v:F_m, suggesting that the reduction in Φ_m at higher E_{gr} is primarily the result of a reduction in PSII reaction centers contributing to photochemistry and is not due to a mechanism diverting absorbed light energy away from photochemistry, such as the xanthophyll cycle.

The decrease in F_v:F_m observed for both strains of *P. antarctica* (Table 2) (13–20%), corresponded well with the decrease in Φ_m (17–23%). The same was not true for *F. cylindrus*, which exhibited a significant decrease in F_v:F_m with higher irradiance (25%) but a much larger decrease in Φ_m (75%). This discrepancy suggests that most of the reduction in Φ_m at high E_{gr} was due to mechanisms other than those causing the loss of functional PSII. The majority of the loss of Φ_m must then be attributed to mechanisms that divert absorbed energy from the pathway of C fixation, including photoprotective mechanisms such as the xanthophyll cycle, in which excess absorbed energy is dissipated as heat, thereby relieving excitation pressure on PSII. Several lines of evidence are consistent with an active xanthophyll cycle in *F. cylindrus*. First, the total amount of pigments of the xanthophyll cycle relative to Chl *a* (DD+DT*) increased 5-fold as E_{gr} increased (Table 1 and Fig. 3A). In addition, the de-epoxidation state of the xanthophyll cycle [DT/(DD+DT)] was positively and strongly correlated to E_{gr} (Fig. 3B). Furthermore, Kropuenske et al. (2009) and Kropuenske et al. (in press) observed increasingly high levels of NPQ, a measure of heat dissipation mediated by the xanthophyll cycle in *F. cylindrus* cultures that were grown under increasingly high irradiance and when shifted from low to high irradiance. There are additional mechanisms that could explain the discrepancy in the declines of F_v/F_m and Φ_m in *F. cylindrus*, such as the Mehler reaction (Mehler 1957), cyclic electron flow around PSI (Heber et al. 1978), and cyclic electron flow within PSII (Miyake and Yokota 2001; Miyake et al. 2002), which have all been shown to reduce excitation pressure on PSII by providing alternate electron pathways that do not lead to reduction of CO_2. In addition, Lomas and Glibert (1999) have proposed that diatoms inhabiting cooler water with abundant nitrate, such as the waters in the Ross Sea (Arrigo et al. 2000), may shunt excess electrons from PSII to the nonnutritional conversion of nitrate to more reduced N forms (nitrite and ammonium) that are subsequently released from the cells to the surrounding medium.

In contrast to *F. cylindrus*, xanthophyll-cycle activity and other pathways dissipating energy appear to be less important for acclimation to high irradiance in *P. antarctica*, in agreement with similar declines in F_v:F_m and Φ_m with increasing E_{gr} and the likely reliance on repair of damaged photosynthetic proteins for maintenance of photosynthetic performance. However, there is evidence for an active xanthophyll cycle in *P. antarctica*. For both strains of *P. antarctica*, DT/(DD+DT) also was positively correlated with E_{gr}, exhibiting a similar response to that observed for *F. cylindrus*. However DD+DT* showed no clear response to changing E_{gr} and DD+DT* was low compared to *F. cylindrus*. Therefore, although our results indicate that the xanthophyll cycle responds to growth irradiance in *F. cylindrus* and *P. antarctica*, they also suggest that the xanthophyll cycle may have a less dynamic photoprotective role in *P. antarctica*. These findings are in agreement with the results of Kropuenske et al. (2009), in which repair of damaged proteins within the reaction center (presumably D1) was found to be of primary importance in maintaining photosynthetic activity in *P. antarctica*, but unimportant in *F. cylindrus*. Instead, *F. cylindrus* relied heavily upon activity of the xanthophyll cycle to maintain photosynthetic performance.

Species distribution in the Ross Sea

Arrigo et al. (1999, 2000) suggested that the observed distribution of phytoplankton species in the Ross Sea is a consequence of taxonomic differences in the ability to exploit the light fields of differing hydrographic regimes. The authors hypothesized that *P. antarctica* is better able to acclimate to lower irradiance than are the bloom-forming diatoms in the Ross Sea and, conversely, that diatoms are better able to acclimate to higher irradiance and are less sensitive to photoinhibition. As a result, the growth of *P. antarctica* is favored in the deeply-mixed waters of the Ross Sea Polynya, where the average irradiance in the mixed layer is much lower than that in the shallowly mixed waters of Terra Nova Bay and the MIZ. In contrast, the growth of diatoms is favored in the Terra Nova Bay and the MIZ, where average irradiance in the mixed layer is higher.

The results of the present study appear to support the hypothesis of Arrigo et al. (1999, 2000), at least

in part. Perhaps the most robust indicator of photoacclimation is growth rate, which integrates all of the catabolic and anabolic activities of the cell, including any changes to these activities that are specifically in response to the availability of irradiance. Over most of the range of E_{gr} examined in this study (25–125 μmol quanta/m^2/s), both *P. antarctica* strains, and in particular the strain isolated from the Ross Sea (*P. antarctica*-1374), grew faster than did *F. cylindrus* (Table 2). However, at high irradiance, μ^{cell} decreased from its maximal value, suggesting that the growth of *P. antarctica* was inhibited at irradiance levels exceeding 65 μmol quanta/m^2/s. Despite the limited dataset used to generate growth-irradiance parameters, our data suggest that the growth rate of *F. cylindrus* should exceed that of *P. antarctica* at irradiances greater than ~250 μmol quanta/m^2/s. Given that prolonged exposure of phytoplankton to irradiance levels in excess 250 μmol quanta/m^2/s is not unlikely within the shallow mixed layers of the Ross Sea during spring and summer (Arrigo et al. 1998c), our observations are consistent with the suggestion of Arrigo et al. (1999, 2000) that differential responses of phytoplankton species to mean ambient irradiance may influence the distribution of these species. It should be noted, however, that our observations of growth and photosynthesis were made under static light conditions and their interpretation may have limits when discussing phytoplankton growth and photoacclimation strategies in natural environments where ambient light conditions can be highly dynamic. In our companion paper by Mills et al. (in press), the hypothesis that the dynamic light regimes characteristic of differing hydrographic conditions may influence species distribution in the Ross Sea was investigated. Their experiments showed that *P antarctica* was able to outcompete *F. cylindrus* when grown under an irradiance regime that simulated deep mixing, while *F. cylindrus* was the superior competitor under an irradiance regime that simulated shallow mixing, consistent with results reported here.

Cullen and MacIntyre (1998) have advanced the concept that phytoplankton have adapted over evolutionary time scales to exploit the degree of stability of light fields generated by specific hydrographic regimes, rather than strictly to the average irradiance field. 'Mixers', phytoplankton adapted to deeply mixed water columns, employ physiological mechanisms that allow them to exploit a highly variable irradiance field. For example, these species maintain photosynthetic capacity that is well in excess of that required for the lower irradiances they experience, allowing them to readily exploit higher irradiance when mixed to shallower depths. At the other extreme, 'layer formers' occupy a narrow vertical distribution and employ physiological mechanisms that exploit a more stable light field, both when light energy is scarce, such as the deep chlorophyll layer or the underside of thick sea ice where acclimation to low irradiance is important, and when light is in excess, such as in a stratified shallow surface layer where protection from the damaging effects of irradiance super-saturating to photosynthesis is required.

Employing the concept of mixers and layer formers provides a useful framework in which to understand the regulation of distribution of microalgal species in the Ross Sea using our observations of photoacclimation under static irradiance conditions. *F. cylindrus* occupies habitats within in the Ross Sea that are more layer-like than those inhabited by *P. antarctica*. Early in the austral spring, well before the onset of ice melt when most of the Ross Sea is covered by ice, *F. cylindrus* commonly is found as a member of a luxuriant microalgal community that is situated in a porous layer at the bottom of the annual sea ice that may attain a thickness of >2 m (Arrigo et al. 2003; Garrison et al. 2003). In this fixed position within the bottom 0.2 m layer of the sea ice, total PAR is more stable, relative to a mixing open-water column, but greatly reduced in magnitude and degraded in spectral quality (SooHoo et al. 1987; Arrigo et al. 1991; Robinson et al.1998). It has been reported that PAR available to bottom-ice microalgal communities in the fast-ice of the Ross Sea is often reduced to less than 1% of surface values (Palmisano et al. 1987) and is restricted to a narrow spectral band centered in the green wavelengths (ca. 550–590 nm) (SooHoo et al. 1987; Arrigo et al. 1991; Robinson et al.1998). To survive in this habitat where light energy is scarce, sea-ice microalgae have adapted to efficiently capture and use the available light for photosynthesis. Studies of the fast ice report E_k values for bottom-ice algae that are <20 μmol quanta/m^2/s, large size of pigment antennae, and increased concentrations of cellular pigments (Lizotte and Sullivan 1991; Robinson et al. 1995). Evidence from the present study indicates that *F. cylindrus* is well suited for growth in the low-light environment of the bottom-ice microalgal community. The species was able to photosynthetically acclimate to an irradiance of 5 μmol quanta/m^2/s, which is <1% of the irradiance that would reach the reach surface waters in the Ross Sea on a cloudless summer day. In addition, cultures acclimated to low light exhibited an enhanced capacity to absorb green light (500–575 nm) that is complimentary to the degraded light spectrum typically found with bottom-ice

habitats (Robinson et al. 1995). It should be noted that *P. antarctica* is also occasionally a conspicuous member of the ice algal community (Arrigo et al. 2003); thus the low E_k measured is consistent with a low-light ice environment. However, Arrigo et al. (2003) showed that *P. antarctica* dominated new ice while *F. cylindrus* dominated older ice, indicating that the diatom may be more suited to long-term survival in the ice. The relatively lower E_k and higher absorption in the green portion of the light spectrum measured here seems to support this.

Later in the Austral spring and summer, as solar warming initiates melting of the annual sea ice in the Ross Sea, phytoplankton blooms form within the shallow mixed layer (~10–20 m) (Arrigo et al. 2000) in the stratified waters of Terra Nova Bay and in the MIZ. *F. cylindrus* and other species that comprise the bottom-ice microalgal community often dominate the species composition of these surface-water blooms, indicating that cells released from the bottom-ice community as the ice melts may act as a seed population for the subsequent phytoplankton blooms (Arrigo et al. 2003). This transition from extremely low irradiance under the sea ice to nearly full sunlight in surface waters represents a challenge to acclimation for a photosynthetic species to overcome. Under high irradiance, *F. cylindrus* appears to lack the ability to adjust its photosynthetic capacity and harvesting of light in a manner that balances acquisition of light energy with photosynthetic requirements. At all but the lowest E_{gr} used in our study, *F. cylindrus* was growing under irradiance conditions that were saturating for photosynthesis, supporting the hypothesis of Cota and Sullivan (1990) that microalgae from low-irradiance habitats under the ice may be obligate shade flora in that they lack the ability to fully photoacclimate to even moderately high irradiance by altering their photosynthetic characteristics. However, field data showing that some ice algae (e.g. *F. cylindrus*) can dominate open-water blooms contradict this hypothesis (Arrigo et al. 2000). As an alternative strategy for survival and growth in the high-light surface waters of the MIZ, it is likely that *F. cylindrus* tolerates supersaturating illumination by employing photoprotective mechanisms, in particular the xanthophyll cycle, which dissipate excess excitation energy and protects PSII from photoinhibitory damage. A similar strategy for acclimation to high irradiance was reported for *Navicula glaciei*, an Antarctic diatom typically found in low-irradiance benthic habitats, but that also may flourish in ponds at the surface of sea ice (Burkholder and Mandelli 1965; Whitaker and Richardson 1980). To survive within the pond habitats at the surface, where irradiance can be 7- to 30-fold greater than E_k values, the species relies upon efficient dissipation of excess excitation energy via the xanthophyll cycle (Robinson et al. 1997). Several studies have shown that diatoms can exhibit very high levels of NPQ (Lavaud et al. 2002, 2004), a consequence of xanthophyll-cycle activity, regularly exhibiting higher levels than do other algal species and vascular plants (Ruban et al. 2004). In addition, Kropuenske et al. (in press) suggested that relaxation of NPQ and the epoxidation of DT to DD after cells are shifted from high to low irradiance conditions can be very slow in *F. cylindrus*, asserting that this trait is characteristic of layer formers acclimated to stable, high-irradiance habitats.

When the central Ross Sea Polynya opens in November, its expansion is apparently driven by the advection of ice away from the region rather than by the melting of ice in place (Arrigo et al. 1998c). Consequently, the water column that is uncovered is weakly stratified and deeply mixed and irradiance may vary from near surface values to values below the compensation point for net growth. Field observations have confirmed that the intense blooms that form in these waters in mid-November through December are consistently dominated by *P. antarctica*, suggesting that this species is uniquely suited to take advantage of the dynamic light field in these waters to gain a competitive advantage. Cullen and MacIntyre (1998) suggested that phytoplankton employing a successful mixer strategy would maintain photosynthetic capacity well in excess of that required for the lower irradiances they experience, allowing them to readily exploit higher irradiances when mixed to shallower depths. In addition, once exposed to high irradiance near the surface, mechanisms would need to be in place to mitigate photoinhibitory damage (Kropuenske et al. 2009).

Several lines of evidence suggest that *P. antarctica* relies on a mixer strategy for photoacclimation. Both strains of *P. antarctica* examined in this study maintained EPC that was 6- to 8-fold in excess of that required for photosynthesis at the lowest E_{gr} (Fig. 3D). In fact, P_m^C was relatively insensitive to E_{gr}, which suggests that the adjustments made to photosynthesis in response to E_{gr} served to maximize the potential for growth, independent of E_{gr}, rather than to balance the harvesting of light energy with the ability to use that energy. Assuming that P–E curves normalized to POC describe the short-term response of growth rate to irradiance, then the

light-saturated growth rate represented by P_m^C, which ranged from 0.6–0.9/d, approached the theoretical maximum growth rate (0.9/d) expected at the 2°C temperature of our incubators (Eppley 1972). In addition, we found little evidence of susceptibility to photoinhibition (β^*) by *P. antarctica* at the levels of light used in this study. Kropuenske et al. (2009) reported that *P. antarctica* was more readily susceptible to photoinhibition than was *F. cylindrus*, but that *P. antarctica* may rapidly repair damage and thereby tolerate high exposure to light. These authors suggested that the combined characteristics of high photosynthetic rate (as phytoplankton mix upward into waters with high irradiance near the surface) and rapid repair of photodamage (as they mix downward away from high light stress) may allow *P. antarctica* to dominate phytoplankton blooms in the central Ross Sea Polynya.

Summary

The Southern Ocean is characterized by its high degree of hydrographic variability. In particular, mixing rates and light levels in the upper mixed layer can differ dramatically from place to place. Phytoplankton growing in these regions must have mechanisms that allow them to exploit the local light environment. Our results help to shed light on the mechanisms employed by the two dominant taxa in the Southern Ocean: diatoms (here *F. cylindrus*) and *P. antarctica*. *F. cylindrus* thrives in stable environments such as shallow mixed layers and under sea ice where levels of light can be very high or very low (Arrigo et al. 1991, 1999). Here, we show that this species copes with high levels of light by maintaining low concentrations of photosynthetic pigments but high levels of photoprotective pigments of the xanthophyll cycle. Although it exhibits relatively low photosynthetic rates and reduced growth rates (Table 2), it is far less susceptible to photoinhibition than is *P. antarctica* (Table 3 and Fig. 3B), allowing it to thrive in the high-light environment that characterizes the MIZ of the Terra Nova Bay polynya in the Ross Sea. In contrast, *P. antarctica* relies less on photoprotection (and has fewer xanthophyll-cycle pigments) and more on repair of photodamage (Kropuenske et al. 2009). It also exhibits higher rates of photosynthesis and growth than does *F. cylindrus* and has much more EPC, particularly at the low light levels that characterize the deep mixed layers where it is most commonly found in the Ross Sea. The potential for photoinhibition is minimized in this deeply mixed environment, allowing *P. antarctica* to form dense blooms that are virtually monospecific.

Understanding the environmental factors that control distributions of the major taxa of phytoplankton in the Southern Ocean is critical if we are to accurately predict the impact of climatic change on their populations. This knowledge eventually can be incorporated into regional and global models, resulting in greatly improved descriptions of the ecology and biogeochemistry of the Southern Ocean and in more reliable predictions.

Funding

This work was supported by the Ocean Carbon Sequestration Research Program, Biological and Environmental Research (BER), US Department of Energy (grant # DE-FG02-04ER63891 and grant # DE-FG02-04ER63896), as well as by NASA (grant # NNG05GR19G) and the National Science Foundation (grant # ANT0732535).

References

Arrigo KR, McClain CR. 1994. Spring phytoplankton production in the western Ross Sea. Science 266:261–3.

Arrigo KR, van Dijken GL. 2004. Annual cycles of sea ice and phytoplankton near Cape Bathurst, southeastern Beaufort Sea, Canadian Arctic. Geophys Res Lett 31:L08304.

Arrigo KR, Sullivan CW, Kremer JN. 1991. A bio-optical model of Antarctic sea ice. J Geophys Res 96:10581–92.

Arrigo KR, van Dijken GL, Bushinsky S. 2008. Primary production in the Southern Ocean, 1997–2006. J Geophys Res 113:C08004.

Arrigo KR, Weiss AM, Smith WO Jr. 1998c. Physical forcing of phytoplankton dynamics in the western Ross Sea. J Geophys Res 103:1007–21.

Arrigo KR, Dunbar RB, Robinson DH, Lizotte MP. 2002. Taxon-specific differences in C/P and N/P drawdown for phytoplankton in the Ross Sea, Antarctica. Geophys Res Lett 29: 2002GL015277.

Arrigo KR, Worthen DL, Schnell A, Lizotte MP. 1998a. Primary production in Southern Ocean waters. J Geophys Res 103:15587–15600.

Arrigo KR, Robinson DH, Dunbar RB, Leventer AR, Lizotte MP. 2003. Physical control of chlorophyll *a*, POC, and PON distributions in the pack ice of the Ross Sea, Antarctica. J Geophys Res 108:3316.

Arrigo KR, Robinson DH, Lizotte MP, Worthen DL, Schieber B. 1998b. Bio-optical properties of the southwestern Ross Sea. J Geophys Res 103:21683–21695.

Arrigo KR, Di Tullio GR, Dunbar RB, Lizotte MP, Robinson DH, van Woert M, Worthen DL. 2000. Phytoplankton taxonomic variability and nutrient utilization and primary production in the Ross Sea. J Geophys Res 105:8827–46.

Arrigo KR, Robinson DH, Worthen DL, Dunbar RB, DiTullio GR, van Woert M, Lizotte MP. 1999. Phytoplankton community structure and the drawdown of nutrients and CO_2 in the Southern Ocean. Science 283:365–7.

Bidigare RR, Frank TJ, Zastrow C, Brooks JM. 1986. The distribution of algal chlorophylls and their degradation products in the Southern Ocean. Deep-Sea Res 33:923–37.

Bricaud A, Stramski D. 1995. Spectral absorption coefficients of living phytoplankton and nonalgal biogenous matter: a comparison between the Peru upwelling area and the Sargasso Sea. Limnol Oceanogr 35:69–75.

Bromwich DH, Carrasco JF, Stearns CR. 1992. Satellite-observations of katabatic-wind propagation for great distances across the Ross Ice Shelf. Monthly Weather Rev 120:1940–9.

Burkholder PR, Mandelli EF. 1965. Productivity of microalgae in Antarctic sea ice. Science 149:872–4.

Caron DA, Dennett MR, Lonsdale DJ, Moran DM, Shalapyonok L. 2000. Microzooplankton herbivory in the Ross Sea, Antarctica. Deep-Sea Res 47 (Pt. II):3249–72.

Cota GF, Sullivan CW. 1990. Photoadaptation, growth and production of bottom ice algae in the Antarctic. J Phycol 26:399–411.

Cullen JJ, MacIntyre JG. 1998. Behavior, physiology and the niche of depth-regulating phytoplankton. In: Anderson DM, Cembella AD, Hallegraeff GM, editors. Physiological ecology of harmful algal blooms. Berlin, Heidelberg: Springer-Verlag. p. 1–21.

Demmig-Adams B. 1990. Carotenoids and photoprotection in plants: a role for the xanthophyll zeaxanthin. Biochimica et Biophysica Acta 1020:1–24.

Demmig B, Winter K, Kruger K, Czygan FC. 1987. Photoinhibition and zeaxanthin formation in intact leaves. Plant Physiol 84:218–24.

DiTullio GR, Smith WO. 1995. Relationship between dimethylsulfide and phytoplankton pigment concentrations in the Ross Sea, Antarctica. Deep-Sea Res 42 (Pt. I):873–92.

DiTullio GR, Grebmeier J, Arrigo KR, Lizotte MP, Robinson DH, Leventer A, Barry J, van Woert M, Dunbar RB. 2000. Rapid and early export of *Phaeocystis antarctica* blooms in the Ross Sea, Antarctica. Nature 404:595–8.

Eppley RW. 1972. Temperature and phytoplankton growth in the sea. Fish Bull 70:1063–85.

Falkowski PG, Owens TG. 1980. Light-shade adaptation: two strategies in marine phytoplankton. Plant Physiol 66:592–5.

Falkowski PG, Raven J. 1997. Aquatic photosynthesis. Blackwell: Oxford. p. 375.

Garrison DL, Jeffries MO, Gibson A, Coale SL, Neenan D, Fritsen C, Okolodkov YB, Gowing MM. 2003. Development of sea ice microbial communities during autumn ice formation in the Ross Sea. Mar Ecol Prog Ser 259:1–15.

Goffart A, Catalano G, Hecq JH. 2000. Factors controlling the distribution of diatoms and *Phaeocystis* in the Ross Sea. J Mar Sys 27:161–75.

Heber U, Egneus H, Hanck U, Jensen M, Koster S. 1978. Regulation of photosynthetic electron-transport and photophosphorylation in intact chloroplasts and leaves of *Spinacia-oleracea* L. Planta 143:41–9.

Johnson Z, Barber RT. 2003. The low-light reduction in the quantum yield of photosynthesis: potential errors and biases when calculating the maximum quantum yield. Photosynthesis Res 75:85–95.

Kana TM, Glibert PM. 1987. Effect of irradiances up to 2000 μE $m^{-2}s^{-1}$ on marine *Synechococcus* WH7803. 2. Photosynthetic responses and mechanisms. Deep-Sea Res 34 (Pt. A):497–516.

Kishino M, Takahashi N, Okami N, Ichimura S. 1985. Estimation of the spectral absorption coefficients of phytoplankton in the sea. Bull Mar Sci 37:634–42.

Kropuenske LR, Mills MM, Van Dijken GL, Bailey S, Robinson DH, Welschmeyer NA, Arrigo KR. 2009. Photophysiology in two major Southern Ocean phytoplankton taxa: photoprotection in *Phaeocystis antarctica* and *Fragilariopsis cylindrus*. Limnol Oceanogr 54:1176–96.

Kropuenske LR, Mills MM, Van Dijken GL, Alderkamp AC, Berg GM, Robinson DH, Welschmeyer NA, Arrigo KR. Strategies and rates of photoacclimation in two major Southern Ocean phytoplankton taxa: *Phaeocystis antarctica* (Haptophyta) and *Fragilariopsis cylindrus* (Bacillariophyceae). J Phycol. In Press.

Lavaud J, Rousseau B, Etienne AL. 2004. General features of photoprotection by energy dissipation in planktonic diatoms (Bacillariophyceae). J Phycol 40:130–7.

Lavaud J, Rousseau B, van Gorkom HJ, Etienne AL. 2002. Influence of the diadinoxanthin pool size on photoprotection in the marine planktonic diatom *Phaeodactylum tricornutum*. Plant Physiol 129:1398–406.

Lewis MR, Smith JC. 1983. A small volume, short-incubation-time method for measurement of photosynthesis as a function of incident irradiance. Mar Ecol Prog Ser 13:99–102.

Liss PS, Malin G, Turner SM, Holligan PM. 1994. Dimethyl sulfide and *Phaeocystis* - A review. J Mar Sys 5:41–53.

Lizotte MP, Sullivan CW. 1991. Photosynthesis-irradiance relationships in microalgae associated with Antarctic pack ice: evidence for in situ activity. Mar Ecol Prog Ser 71:175–84.

Lomas MW, Glibert PM. 1999. Interactions between NH_4^+ and NO_3^- uptake and assimilation: comparison of diatoms and dinoflagellates at several growth temperatures. Mar Biol 133:541–51.

Macintyre HL, Kana TM, Anning T, Geider RJ. 2002. Photoacclimation of photosynthesis irradiance response curves and photosynthetic pigments in microalgae and cyanobacteria. J Phycol 38:17–38.

Mehler AH. 1957. Studies on reactions of illuminated chloroplasts. I. Mechanism of the reduction of oxygen and other Hill reagents. Arch Biochem Biophys 33:65–77.

Melis A. 1999. Photosystem-II damage and repair cycle in chloroplasts: what modulates the rate of photodamage in vivo? Trends Plant Sci 4:130–5.

Mills MM, Kropuenske LR, van Dijken GL, Alderkamp A-C, Berg GM, Robinson DH, Welschmeyer NA, Arrigo KR. (In press). Photophysiology in two major Southern Ocean phytoplankton taxa: Photosynthesis and growth of Phaeocystis antarctica (Prymnesiophyceae) and Fragilariopsis cylindrus (Bacillariophyceae) under simulated mixed layer irradiance. J Phycol.

Mitchell BG, Kiefer DA. 1988. Chlorophyll *a* specific absorption and fluorescence excitation spectra for light-limited phytoplankton. Deep Sea Res 35:639–89.

Miyake C, Yonekura K, Kobayashi Y, Yokota A. 2002. Cyclic electron flow within PSII functions in intact chloroplasts from spinach leaves. Plant Cell Physiol 43:951–7.

Moore JK, Abbott MR. 2000. Phytoplankton chlorophyll distributions and primary production in the Southern Ocean. J Geophys Res 105:28709–22.

Morel A, Bricaud A. 1981. Theoretical results concerning light absorption in a discrete medium, and application to specific absorption of phytoplankton. Deep-Sea Res 28:1375–93.

Morel FMM, Rueter JG, Anderson DM, Guillard RRL. 1979. Aquil - Chemically defined phytoplankton culture-medium for trace-metal studies. J Phycol 15:135–41.

Nishiyama Y, Allakhverdiev SI, Murata N. 2006. A new paradigm for the action of reactive oxygen species in the photoinhibition of photosystem II. Biochim Biophys Acta 1757:742–9.

Olaizola M, Yamamoto HY. 1994. Short-term response of the diadinoxanthin cycle and fluorescence yield to high irradiance in *Chaetoceros muelleri* (Bacillariophyceae). J Phycol 30:606–12.

Olaizola M, LaRoche J, Kolber Z, Falkowski PG. 1994. Non-photochemical quenching and the diadinoxanthin cycle in a marine diatom. Photosyn Res 41:357–70.

Palmisano AC, SooHoo JB, Moe RL, Sullivan CW. 1987. Sea ice microbial communities VII. Changes in under-ice spectral irradiance during the development of Antarctic sea ice microalgal communities. Mar Ecol Prog Ser 35:165–73.

Platt T, Gallegos CL, Harrison WG. 1980. Photoinhibition of photosynthesis in natural assemblages of marine phytoplankton. J Mar Res 38:687–701.

Price NM, Harrison GI, Hering JG, Hudson RJ, Nirel PMV, Palenik B, Morel FMM. 1989. Preparation and chemistry of the artificial algal culture medium Aquil. Biol Oceanogr 6:443–61.

Rhodes RH, Bertler NAN, Baker JA, Sneed SB, Oerter H, Arrigo KR. 2009. Sea ice variability and primary productivity in the Ross Sea, Antarctica, from methylsulphonate snow record. Geophys Res Lett 36:L10704.

Robinson DH, Kolber Z, Sullivan CW. 1997. Photophysiology and photoacclimation in surface sea ice algae from McMurdo Sound, Antarctica. Mar Ecol Prog Ser 147:243–56.

Robinson DH, Arrigo KR, Iturriaga R, Sullivan CW. 1995. Adaptation to low irradiance and restricted spectral distribution by Antarctic microalgae from under-ice habitats. J Phycol 31:508–20.

Robinson DH, Arrigo KR, DiTullio GR, Lizotte MP. 2003. Evaluating photosynthetic carbon fixation during *Phaeocystis antarctica* blooms. In: DiTullio GR, Dunbar RB, editors. Biogeochemistry of the Ross Sea. Ant Res Ser 78:77–91.

Robinson DH, Arrigo KR, Gosselin M, Kolber Z, Sullivan CW. 1998. Evidence for nutrient limitation in the platelet ice algal community in McMurdo Sound, Antarctica. J Phycol 34:788–97.

Roesler CS, Perry MJ, Carder KL. 1989. Modeling in situ phytoplankton absorption from total absorption-spectra in productive inland marine waters. Limnol Oceanogr 34:1510–23.

Ruban VA, Lavaud J, Rousseau B, Gugliemi G, Horton P, Etienne AL. 2004. The super-excess energy dissipation in diatom algae: Comparative analysis with higher plants. Photosyn Res 82:165–75.

Smith WO Jr, Gordon LI. 1997. Hyperproductivity of the Ross Sea (Antarctica) Polynya during austral spring. Geophys Res Lett 24:233–6.

Smith WO, Nelson DM, Mathot S. 1999. Phytoplankton growth rates in the Ross Sea, Antarctica, determined by independent methods: temporal variations. J Plank Res 21:1519–36.

Sommer U. 1989. Maximal growth rates of Antarctic phytoplankton: only a weak dependence of size. Limnol Oceanogr 34:1109–12.

SooHoo JB, Palmisano AC, Kottmeier ST, Lizotte MP, SooHoo SL, Sullivan CW. 1987. Spectral light absorption and quantum yield of photosynthesis in sea ice microalgae and a bloom of *Phaeocystis pouchetii* from McMurdo Sound, Antarctica. Mar Ecol Prog Ser 39:175–89.

Sweeney C, et al. 2000. Nutrient and carbon removal ratios and fluxes in the Ross Sea, Antarctica. Deep-Sea Res 47:3395–422.

Vaillancourt RD, Marra J, Barber RT, Smith WO. 2003. Primary productivity and in situ quantum yields in the Ross Sea and Pacific sector of the Antarctic Circumpolar Current. Deep-Sea Res 50 (Pt II):559–78.

Van Hilst CM, Smith WO Jr. 2002. Photosynthesis/irradiance relationships in the Ross Sea, Antarctica, and their control by phytoplankton assemblage composition and environmental factors. Mar Ecol Prog Ser 226:1–12.

Whitaker TM, Richardson MG. 1980. Morphology and chemical composition of a natural population of an ice-associated Antarctic diatom *Navicula glaciei*. J Phycol 16:250–7.

Zapata M, Rodriguez F, Garrido JL. 2000. Separation of chlorophylls and carotenoids from marine phytoplankton: a new HPLC method using a reversed phase C-8 column and pyridine-containing mobile phases. Mar Ecol Prog Ser 195:29–45.